GA–A26785

GIANT SAWTEETH IN DIII-D AND THE QUASI-INTERCHANGE MODE

by
A.D. TURNBULL, M. CHOI, and L.L. LAO

NOVEMBER 2010

GENERAL ATOMICS

DISCLAIMER

GA–A26785

GIANT SAWTEETH IN DIII-D AND THE QUASI-INTERCHANGE MODE

by
A.D. TURNBULL, M. CHOI, and L.L. LAO

This is a preprint of a paper to be presented at the 37th European Physical Society Conference on Plasma Physics, June 21-25, 2010, Dublin, Ireland and to be published in the *Proceedings.*

Work supported in part by
the US Department of Energy
under DE-FG03-95ER54309

GENERAL ATOMICS PROJECTS 03726
NOVEMBER 2010

GENERAL ATOMICS

Giant Sawteeth in DIII-D and the Quasi-Interchange Mode

A.D. Turnbull, M. Choi, and L.L. Lao

General Atomics, PO Box 85608, San Diego, California 92186, USA

Reconstructed discharge equilibria in DIII-D provide a unique opportunity to follow and compare the time evolution of three discharges, with very different sawtooth characteristics, in detail over several sawtooth cycles. The discharges comprised low beta oval shaped and bean shaped discharges [1] and a single-null ion cyclotron resonance frequency (ICRF)-heated discharge [2]. Two distinct types of crash are observed, differing in the coupling of the crash in the electron temperature and the poloidal field changes. The crash in the bean discharge follows the conventional Kadomtsev model [3]. However, the oval and ICRF-heated discharges exhibit a decoupling of the time scale of the crash in the central electron temperature, T_e, from the poloidal field changes, B_σ, that is inconsistent with this model. This is difficult to explain within the context of the Kadomtsev model but is consistent with a quasi-interchange model [4]. The observations can be reconciled by invoking the model of an instability being driven through a stability threshold [5].

The most notable feature of the q profile evolution is the steady drop in the core below one and the return to $q_0 \sim 1$ at the crash in each case, consistent with the conventional picture of the sawtooth cycle. This is the common behavior of all DIII-D sawtoothing discharges for which the multiple channel motional Stark effect (MSE) diagnostic permits a valid reconstruction of the q profile. Also notable, is the formation of an off-axis minimum, q_{min}, in q immediately after the crash. The reconstructed equilibrium q_0 and q_{min} are shown in Fig. 1 for each case: (a) the bean discharge #118162, (b) the oval discharge #118164, and (c) the ion cyclotron resonance heated (ICRH) discharge #96043, covering the full sequence of sawtooth cycles examined. The crash times are indicated by the solid vertical lines and the dashed lines straddle MHD relaxation events. These events appear to be ubiquitous in DIII-D sawtoothing discharges. The respective cross sections are also shown. For the bean discharge shown in Fig. 1(a), the off-axis minimum persists through the relaxation events [Fig. 1(b)], but for the oval, it persists until the subsequent crash. Also, q_0 drops considerably further in the bean case, to around 0.85 than in the oval where it reaches only 0.95. The behavior of the q profile for the ICRF-heated discharge is intermediate between these.

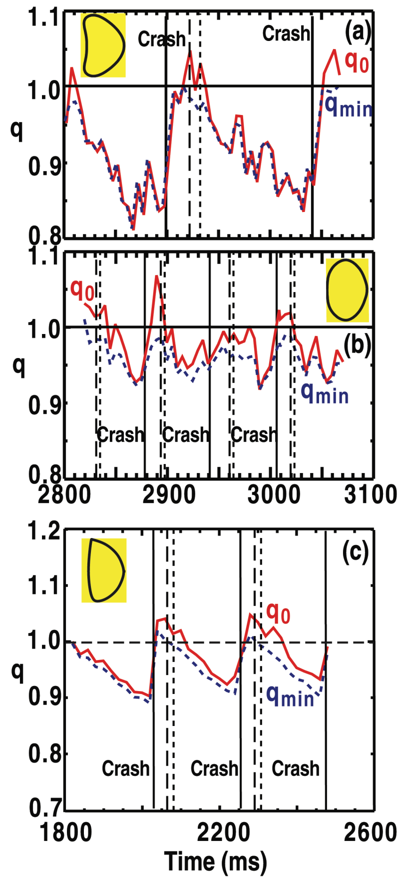

Fig. 1. Time variation of q_0 and q_{min} through several sawtooth cycles for (a) discharge #118162, (b) discharge #118164, and (c) discharge #96043. In each case, the crash times are indicated by the vertical lines and the MHD relaxation events are straddled by the dashed vertical lines.

A key difference noted in Ref. [1] between the bean and oval discharges is that no reconnection event associated with the crash was observed in the oval whereas a distinct reconnection with subsequent island was observed in the bean discharge. Other details of the crash events were also different. In the bean, both the crash in T_e and the change in B_θ resetting q_0 (poloidal field crash) are both fast. The crash in T_e was less than 100 μs. The crash in B_θ was not resolvable within the 500 μs, time resolution of the MSE diagnostic. In contrast, for the oval, the crash in T_e was also fast — less than 100 μs, as in the bean — but the change in B_θ was of the order of 5 ms, and so at least an order of magnitude slower. In addition, the oval discharge exhibited a growing precursor oscillation before each crash. For the bean there was only a successor oscillation.

The crash in the ICRF-heated discharge was significantly different from that in normal DIII-D sawtoothing discharges in that it was much larger [2], resembling the so-called giant sawteeth seen in ICRH discharges in JET [6]. In discharge #96043, the giant sawtooth phase was initiated in response to the application of additional ICRF heating in a neutral-beam heated discharge. Further analysis showed that in this case, the change in the B_θ signal was also much slower than the crash in T_e.

The ideal MHD stability of each reconstructed discharge equilibrium was computed using the GATO code [7]. The results for the ideal growth rate $\gamma_I \tau_A$ are summarized in Fig. 2. The stability was computed assuming the DIII-D vacuum vessel as a perfectly conducting boundary condition but shown also is the result for a wall on the plasma boundary.

Neither the bean discharge nor the ICRF-heated discharge follows the conventional picture of degrading ideal stability with decreasing q_0 through the ramp phase. The ideal growth rate for the bean drops rapidly about a third of the way into the cycle, not long after the q profile becomes monotonic. For the last two thirds of the ramp phase, the ideal growth rate hovers around marginal stability, as indicated by the fact that at times the respective equilibria are stable when the wall is moved on to the plasma boundary. For the ICRF-heated discharge, $\gamma_I \tau_A$ slowly decreases through the ramp. Thus the bean has a quite different time evolution of the ideal stability and the time evolution seems counterintuitive with respect to the sawtooth trigger as well as with respect to the significantly lower q_0.

Using the ideal growth rates obtained in Fig. 2, the Porcelli model [8] is qualitatively consistent with the crash onset within the expected uncertainties in the model and in the equilibrium reconstructions for the three discharges. For the ICRF-heated discharge, the Porcelli model even quantitatively reproduces the crash trigger [2]. For the oval and ICRF-heated discharges, the trigger occurs when the ideal mode free energy exceeds the non-ideal stabilizing contributions. For the bean, the ideal

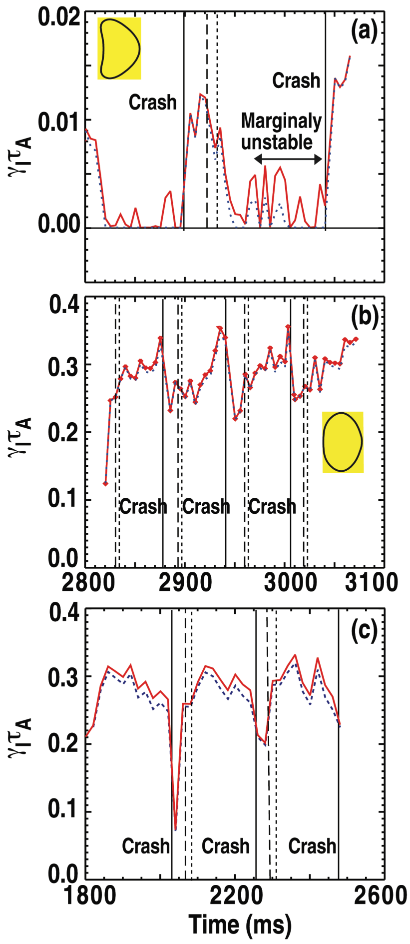

Fig. 2. Time variation of γ_I through several sawtooth cycles for (a) discharge #118162, (b) discharge #118164, and (c) discharge #96043. The solid curves are the result using the DIII-D vacuum vessel as a boundary condition. The dashed curves in (a) and (b) are the result for a wall on the plasma surface. In each case, the crash times are indicated by the vertical lines and the MHD relaxation events are straddled by the dashed vertical lines.

contribution is essentially zero and the trigger can only occur when the destabilizing resistive contributions are sufficiently large. In all three discharges, however, the trigger occurs predominantly because the stabilizing kinetic contributions from both thermal and energetic ions are reduced as a result of the local shear at $q = 1$ increasing through the ramp.

Experimentally, there are then two distinct crash types: one such as in the bean discharge where the timescales for the T_e collapse and the crash in B_θ are apparently coupled, and the other where they are uncoupled and occur on widely different time scales, with a fast T_e crash and much slower B_θ crash. These correspond to distinctly different behaviour in the ideal growth rates of Fig. 2. According to the Kadomtsev model, [3] the fast collapse in T_e inside $q = 1$ occurs as the core moves rigidly out and rams into the $q = 1$ surface. The crash in T_e is then coupled with reconnection at the $q = 1$ surface, and q is reset back to a value near one in the core. A key feature is that the return flow occurs in the narrow reconnection layer and the time scales for the crash in T_e and the reconnection are directly coupled and both fast as a result of the narrowness of the reconnection layer.

An important clue to explaining the different crash types is that for the oval there is some experimental evidence [1,9] that the underlying mode is a quasi-interchange mode. The evidence derives from an analysis of the phase of the crash precursor [1] and from analysis of the effects of the crash on the fast ion distribution; the fast ion redistribution in the oval is consistent with a quasi-interchange mode with no fast reconnection [9]. Additionally, JET soft x-ray measurements [10] for the giant sawteeth in the giant sawtooth experiments found the convective nonlinear flow patterns anticipated from a linear quasi-interchange mode.

The quasi-interchange mode was first proposed by Wesson as an explanation of observations in JET [4]. This model invokes a different dynamics from the Kadomtsev model, whereby the rapid crash in T_e results from the ideal MHD motion of the cold exterior plasma into the core but the B_θ evolution that resets q_0 occurs over a much longer time scale through part of the subsequent ramp period. This is consistent with the experimental observation in the oval and ICRF-heated discharge discussed here.

Taken at face value, the ideal stability calculations for the reconstructed discharge equilibria in this study also reveal the underlying mode to be a quasi-interchange-like mode with a broad return flow pattern at the crash times in the oval and ICRF-heated discharges, but a conventional internal kink with the return flow concentrated entirely at the $q = 1$ surface at the crash time for the bean discharge. These are shown in Fig. 3 for the bean and oval discharges; the flow pattern for the ICRF-heated discharge is similar to that in Fig. 3(b). For a mode with a broad return flow as in Fig. 3(b), the Wesson model, which decouples the two time scales, can apply.

While suggestive, the calculated mode structures included the finite inertia of the ideal mode with no non-ideal stabilization. In the discharges, the effective linear growth rate is expected to be reduced to near zero due to the non-ideal stabilization effects, as described in principle by the Porcelli model, and the modes should therefore be inertia free. For the bean, the ideal mode itself is near marginal and, consistent with Fig. 3(a), does exhibit the top-hat structure expected for an inertia-free mode. In the oval and ICRF-heated discharges, the broader mode structures are a result of the broadening due to the finite inertia [11]. If the inertia is removed, the mode for the oval discharge reverts to the conventional top-hat internal kink and the Kadomtsev model should apply.

It is not easy to reconcile the inertia-free modes with the observed differences in the crash dynamics. On the other hand, invoking the full inertia eigenfunction is difficult to justify. One possible resolution is to invoke the conjecture that the mode is being driven through the stability boundary [5]. In that case, the mode has an effective finite growth rate. An important confirmation pointing to this is the observation that the oval discharge exhibits an $n = 1$ precursor. In this scenario, because the bean discharge is near marginal with respect to ideal stability, the inertia remains negligible as the equilibrium evolves beyond the marginal point. For the oval and ICRF-heated discharge, the ideal contribution increases rapidly and inertia becomes important. However, to apply the model in Ref [5] requires the rate at which the growth rate changes. In Ref. [5], it is assumed that this is the rate of change in β and that γ scales with $\beta^{1/2}$. In the present case, the change in the stability boundary is dependent on more subtle effects, even in the ideal limit.

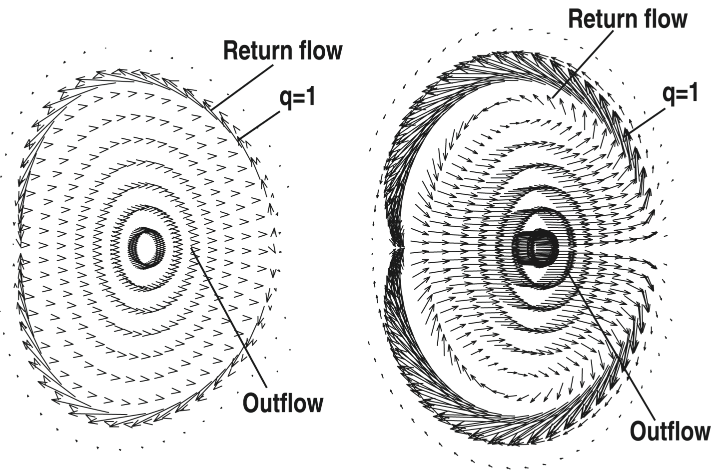

Fig. 3. Linear instability flow pattern showing an expanded view of the core inside and around the q=1 surface for (a) the bean discharge and (b) oval discharge.

From the experimental data, the change in B_θ for the bean is only resolved to within 500 ms and may therefore also be up to a factor five longer than the T_e collapse. In that case, the bean also would have some of the Wesson-like crash characteristics. The calculations can support a small broadening of the linear mode flow patterns within the uncertainties in the equilibrium reconstruction.

The MHD relaxation events may add some additional clues to the crash dynamics. During these events, the underlying ideal mode is also clearly a quasi-interchange in all three cases and the events appear to be quite similar to the oval sawtooth crash itself. There is a distinct difference, however. The data shown in Fig. 1 is consistent with the presence of two $q = 1$ surfaces present, indicated by $q_{\min} < 1$ and $q_0 > 1$ at the onset of the event, and with the loss of the innermost one at the termination of the event as q_0 drops below one, in contrast to the actual sawtooth crashes where q_0 is reset back to $q \sim 1$. While the data is only suggestive due to the significant uncertainties, it seems natural to conjecture that the observed relaxation events are a manifestation of the loss of this surface.

This work was supported by the US Department of Energy under DE-FG03-95ER54309.

[1] E.A. Lazarus, et al., Phys. Plasmas **14**, 055701 (2007).
[2] M. Choi, et al., Phys. Plasmas **14**, 112517 (2007).
[3] B.B. Kadomtsev, Sov. J. Plasma Phys. **1**, 389 (1975).
[4] J.A. Wesson, Plasma Phys. Control. Fusion, **28**, 243, (1987).
[5] J.D. Callen, C.C. Hegna, B.W. Rice, E.J. Strait, and A.D. Turnbull, Phys. Plasmas **6**, 2963 (1999).
[6] D.J. Campbell, et al., Phys. Rev. Lett. **60**, 2148 (1988).
[7] L.C. Bernard, F.J. Helton, R.W. Moore, Comput. Phys. Commun. **24,** 377 (1981).
[8] F. Porcelli, D. Boucher, M.N. Rosenbluth, Plasma Phys. Control. Fusion **38**, 2163 (1996).
[9] C. Muscatello, private communication (2009).
[10] A.W. Edwards, et al., Phys. Rev. Lett. **57**, 210, (1986).
[11] M.N. Rosenbluth, R.Y. Dagazian, and P.H. Rutherford, Phys. Fluids **16**, 1894 (1973).